

Atomic layer deposition of ZnO on ultralow-density nanoporous silica aerogel monoliths

S. O. Kucheyev,^{a)} J. Biener, Y. M. Wang, T. F. Baumann, K. J. Wu, T. van Buuren, A. V. Hamza, and J. H. Satcher, Jr.
Lawrence Livermore National Laboratory, Livermore, California 94550

J. W. Elam and M. J. Pellin
Argonne National Laboratory, Argonne, Illinois 60439

(Received 10 September 2004; accepted 19 January 2005; published online 18 February 2005)

We report on atomic layer deposition of an ~ 2 -nm-thick ZnO layer on the inner surface of ultralow-density ($\sim 0.5\%$ of the full density) nanoporous silica aerogel monoliths with an extremely large effective aspect ratio of $\sim 10^5$ (defined as the ratio of the monolith thickness to the average pore size). The resultant monoliths are formed by amorphous-SiO₂ core/wurtzite-ZnO shell nanoparticles which are randomly oriented and interconnected into an open-cell network with an apparent density of $\sim 3\%$ and a surface area of ~ 100 m² g⁻¹. Secondary ion mass spectrometry and high-resolution transmission electron microscopy imaging reveal excellent uniformity and crystallinity of ZnO coating. Oxygen *K*-edge and Zn *L*₃-edge soft x-ray absorption near-edge structure spectroscopy shows broadened *O p*- as well as Zn *s*- and *d*-projected densities of states in the conduction band. © 2005 American Institute of Physics. [DOI: 10.1063/1.1870122]

Aerogels are nanoporous solids derived from highly cross-linked wet gels by drying them under supercritical conditions.¹ These solids are formed by nanometer size particles randomly interconnected into an open-cell network typically with a large degree of mesoporosity ($\geq 80\%$) and high surface area (≥ 50 m² g⁻¹). Most previous studies have focused on amorphous silica (SiO₂) aerogels, first synthesized by Kistler a number of decades ago.² However, recent advancements in the sol-gel technology have led to a successful synthesis of a range of metal oxide aerogels including oxides of Ti, V, Cr, Fe, Sn, and Ru.¹ The development of such metal-oxide aerogels has been fueled by their numerous potential technological applications based on unique properties of aerogels. Indeed, extremely low densities and high surface areas of monolithic aerogels open up an opportunity to improve the performance of various metal-oxide-based devices, including gas- and biosensors, batteries, heterogeneous catalysis devices, as well as low dielectric constant materials for integrated circuits (so-called low-*k* dielectrics).^{1,3}

However, some metal-oxide systems, such as ZnO, are currently not amenable to the sol-gel method used to synthesize aerogels.¹ Such low-density and high-surface area nanoporous ZnO monoliths would be very attractive for the development of a new generation of ZnO-based gas-sensing and catalytic devices, which have received extensive research efforts in the past several years.⁴ In this letter, we report on a synthesis of monolithic aerogels by atomic layer deposition (ALD) of ZnO on the inner surface of ultralow-density silica aerogels. ALD is a unique tool to deposit ultrathin films of a wide variety of materials, including metal oxides, on curved surfaces with a high-aspect ratio such as the inner surface of a nanoporous solid.⁵ The self-limiting nature of the ALD process enables uniform non-line-of-sight deposition in a combination with atomic level control of the layer thickness. Our results also demonstrate that ALD is a very attractive tool for the synthesis of *monolayer catalysts*

and gas sensors based on well-developed nanoporous monolithic material systems such as silica, alumina, and carbon aerogels,¹ with desirable high surface areas, low densities, and good mechanical properties.

Amorphous SiO₂ aerogels were synthesized at Lawrence Livermore National Laboratory. The details of aerogel synthesis can be found in Ref. 6. Reference bulk wurtzite ZnO single crystals were (001) oriented and O face polished, obtained from Cermet, Inc. The ALD was performed in a viscous flow reactor operated in a quasistatic mode at Argonne National Laboratory.⁷ Several-mm-thick monolithic silica aerogels with a density of 10 mg cm⁻³ were coated with an ~ 2 -nm-thick ZnO layer by alternating 300 s exposures to diethyl zinc/H₂O at 177 °C at a pressure of 10 Torr. Prior to ZnO deposition, an ~ 0.26 -nm-thick nucleation layer of amorphous Al₂O₃ was deposited in two cycles of trimethyl aluminum/H₂O at the same conditions as ZnO. The purpose of such an Al₂O₃ nucleation layer was to prepare a densely hydroxylated surface to minimize any nucleation delay of the subsequent ALD of ZnO.⁸ Between each exposure, the reactor was evacuated below 0.24 Torr and then purged with ultrahigh purity Ar for 200 s.

Spatial and depth uniformity of the ZnO film was studied by time-of-flight secondary ion mass spectrometry (TOF-SIMS) in a TRIFT III (Physical Electronics) instrument equipped with a Ga⁺ ion gun. The bulk densities of aerogels were determined by measuring the dimensions and mass of monolithic samples. Surface area determination and pore volume analysis were performed by Brunauer-Emmett-Teller (BET) and Barrett-Joyner-Halenda (BJH) methods using an ASAP 2000 surface area analyzer (Micromeritics Instrument Corp.), as described in more detail elsewhere.⁶ The microstructure was studied by bright-field high-resolution transmission electron microscopy (HRTEM) in a Philips CM300FEG transmission electron microscope operating at 300 kV.

Soft x-ray absorption near-edge structure (XANES) spectroscopy experiments were performed (at 300 K) at undulator beamline 8.0 at the Advanced Light Source,

^{a)} Author to whom correspondence should be addressed; electronic mail: kucheyev@llnl.gov

TABLE I. Some properties of amorphous silica aerogels before and after the deposition of wurtzite ZnO.

	Apparent density (mg cm^{-3})	Porosity (%)	Surface area ($\text{m}^2 \text{g}^{-1}$)	Pore volume ($\text{cm}^3 \text{g}^{-1}$)
Uncoated	10	99.5	352	2.8
ZnO coated	150	97.1	102	0.92

Lawrence Berkeley National Laboratory. The details of the beamline have been reported in Ref. 9. Aerogels were pressed into an In foil and mounted on the sample holder. The surface normal of ZnO single crystals and In foils was at an angle of 40° relative to the incident x-ray beam axis. Spectra were obtained by recording (i) the total fluorescence yield (TFY), measured with a negatively biased channeltron and (ii) the total electron yield (TEY), measured by monitoring the total sample photocurrent. Measurements in TEY and TFY modes probe the material properties averaged over the first ~ 10 – 20 nm and several hundred nanometers from the sample surface, respectively.¹⁰ The incoming radiation flux was monitored by the total photocurrent produced in a clean Au mesh inserted into the beam. After a constant background subtraction, all XANES spectra were normalized to the post-edge step heights.

Table I summarizes apparent densities, porosities, and results of the BET/BJH nitrogen adsorption/desorption analysis for uncoated (as-synthesized) and ZnO coated silica aerogels. It is seen from Table I that the uncoated material is highly porous with the surface area comparable to that reported previously for silica aerogels of similar densities.¹ Table I also shows that coating with ZnO results in an expected decrease in porosity and surface area and an associated decrease in the average pore volume. However, coated aerogels still exhibit desirable high surface area and ultralow density. Figure 1 shows typical TOF-SIMS images of fractured aerogels, illustrating excellent uniformity of both the

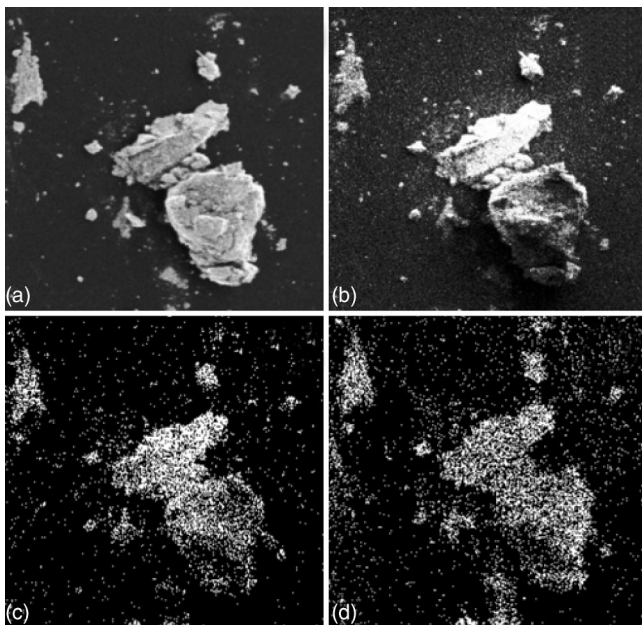


FIG. 1. TOF-SIMS images of fractured ZnO coated silica aerogels. Images are formed by the following SIMS channels: (a) secondary electron, (b) total ion, (c) ZnO^+ , and (d) Al^+ channels. All four images are of the same magnification. The horizontal field width of each image is $10 \mu\text{m}$.

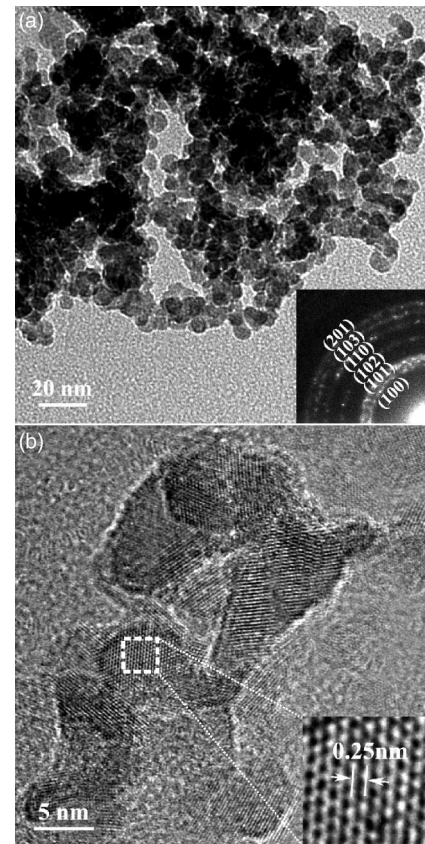


FIG. 2. HRTEM images of a ZnO coated silica aerogel at different magnifications. The inset in (a) shows a selected-area diffraction pattern taken from multiple nanoparticles forming the aerogel. The pattern is indexed to the wurtzite phase of ZnO. The inset in (b) shows a Fourier-filtered image of an individual nanoparticle, illustrating excellent crystallinity of ZnO.

top ZnO layer and the Al_2O_3 nucleation layer. This result has also been verified by TOF-SIMS depth profiles (figures are not shown).

The morphology of coated aerogels is further illustrated in a low-magnification HRTEM image in Fig. 2(a), showing that the aerogel skeleton is formed by ~ 5 – 8 nm particles interconnected into a tree-like structure. A Gaussian fit to the size distribution of nanoparticles from Fig. 2(a) has a maximum at 7.0 nm and a halfwidth of 2.5 nm. The inset in Fig. 2(a) shows a selected-area diffraction pattern (SAD) taken from multiple nanoparticles forming the aerogel skeleton. This SAD pattern is indexed to the wurtzite phase of ZnO, and no contribution from other possible phases of ZnO [such as the rocksalt phase, which has shown to be metastable at ambient conditions for nanocrystalline ZnO (Ref. 11)] has been identified.¹² In addition, the continuous SAD ring pattern suggests that the wurtzite nanocrystals forming the aerogel solid network are randomly oriented.

The orientation and structure of the nanocrystalline ALD ZnO layer are better illustrated in a high-magnification HRTEM image in Fig. 2(b). A Fourier-filtered image of an individual nanoparticle shown in the inset in Fig. 2(b) illustrates excellent crystallinity. The presence of a crystalline phase of ZnO after deposition at a relatively low temperature (i.e., 177°C) is consistent with a large ionicity of Zn-O bonds (0.616 according to Phillips¹³). Due to such a large ionicity, an amorphous phase of stoichiometric ZnO appears to be unstable at ambient conditions¹⁴ and has not been reported.^{15,16}

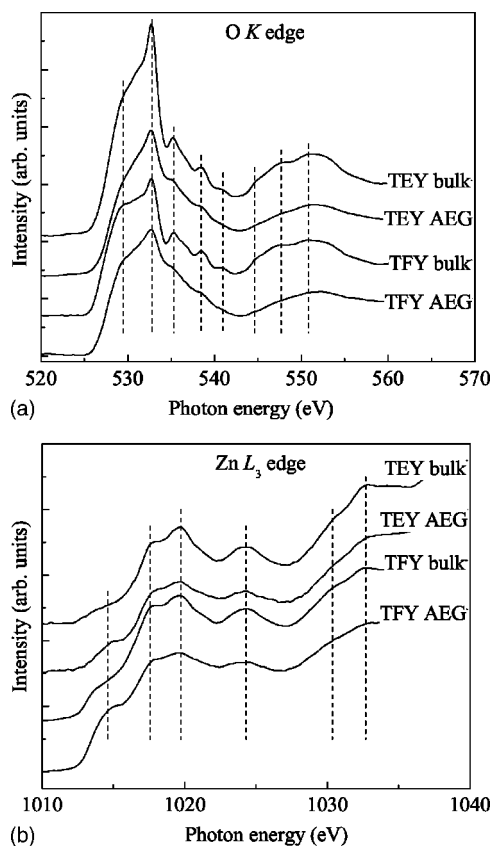


FIG. 3. Total electron yield (TEY) and total fluorescence yield (TFY) O K -edge (a) and Zn L_3 -edge (b) XANES spectra of ZnO coated silica aerogels (labeled as "AEG") and ZnO single crystals (labeled as "bulk").

Since gas-sensing and catalytic applications of ZnO are based on the specific electronic properties, we have studied the electronic structure of ZnO coated aerogels by XANES spectroscopy. Figure 3 gives a comparison of TEY and TFY O K -edge [Fig. 3(a)] and Zn L_3 -edge [Fig. 3(b)] XANES spectra of ZnO coated aerogels and ZnO single crystals. Oxygen K -edge spectra of single crystal ZnO are in general agreement with results of previous studies,^{17–21} but we are not aware of any reports on Zn $L_{2,3}$ -edge XANES characterization of ZnO. If core-hole and electron correlation effects are ignored, such O K -edge spectra essentially map the O p -projected density of empty states, while Zn L_3 -edge spectra reflect transitions of Zn $2p_{3/2}$ core electrons into Zn s - and d -projected electronic states in the conduction band.

Figure 3 shows that ZnO coated aerogels exhibit the same spectral features as those observed for single crystal ZnO standards. However, Fig. 3 also reveals that relative peak intensities are different for single crystals and aerogels, and all spectral features of aerogels are broadened for both (surface sensitive) TEY and (bulk sensitive) TFY spectra. Such a spectral broadening has previously been observed in XANES studies of other semiconductor nanoparticles (such as InAs, CdSe, and TiO₂) of similar sizes.^{22–24} However, the interpretation of this effect is not straightforward since a number of factors, which are difficult to control, can affect XANES spectra. These factors include surface reconstruction and passivation, stress, particle-particle and particle-support interaction, quantum confinement, and charging. Hence, the effects of the ZnO particle size and surface atom fraction on

the electronic density of states currently warrant additional systematic studies.

In conclusion, we have reported on a synthesis of monolithic aerogels by atomic layer deposition of ZnO on the inner surface of ultralow-density silica aerogel monoliths. Such core/shell monoliths have an apparent density of $\sim 3\%$ and a surface area of $\sim 100 \text{ m}^2 \text{ g}^{-1}$. This study demonstrates that ALD is a very attractive tool for the fabrication of monolayer catalysts and gas sensors based on well-developed, robust nanoporous monolithic material systems such as silica, alumina, and carbon aerogels.

Work at LLNL was performed under the auspices of the U.S. DOE by the University of California, LLNL under Contract No. W-7405-Eng-48. The ALS is supported by the Director, Office of Science, Office of BES, Materials Sciences Division, of the U.S. DOE under Contract No. DE-AC03-76SF00098 at LBNL.

¹See, for example, recent reviews by N. Hüsing and U. Schubert, *Angew. Chem., Int. Ed.* **37**, 22 (1998); T. F. Baumann, A. E. Gash, G. A. Fox, J. H. Satcher, Jr., and L. W. Hrubesh, in *Handbook of Porous Solids*, edited by F. Schuth, K. S. W. Sing, and J. Weitkamp (Wiley-VCH, Weinheim, 2002); D. R. Rolison, *Science* **299**, 1698 (2003).

²S. S. Kistler, *Nature (London)* **127**, 741 (1931).

³R. D. Miller, *Science* **286**, 421 (1999).

⁴See, for example, a recent review by S. J. Pearton, D. P. Norton, K. Ip, and Y. W. Heo, *J. Vac. Sci. Technol. B* **22**, 932 (2004).

⁵See, for example, a recent review by J. E. Crowell, *J. Vac. Sci. Technol. A* **21**, 88 (2003).

⁶L. W. Hrubesh, T. M. Tillotson, and J. F. Poco, in *Chemical Processing of Advanced Materials*, edited by L. L. Hench and J. K. West (Wiley, New York, 1992), p. 19.

⁷J. W. Elam, D. Routkevitch, P. P. Mardilovich and S. M. George, *Chem. Mater.* **15**, 3507 (2003).

⁸J. W. Elam, C. A. Wilson, M. Schuisky, Z. A. Sechrist, and S. M. George, *J. Vac. Sci. Technol. B* **21**, 1099 (2003).

⁹J. J. Jia, T. A. Callcott, J. Yurkas, A. W. Ellis, F. J. Himpsel, M. G. Samant, J. Stohr, D. L. Ederer, J. A. Carlisle, E. A. Hudson, L. J. Terminello, D. K. Shuh, and R. C. C. Perera, *Rev. Sci. Instrum.* **66**, 1394 (1995).

¹⁰J. Stöhr, *NEXAFS Spectroscopy* (Springer, Berlin, 1996).

¹¹F. Decremps, J. Pellicer-Porres, F. Datchi, J. P. Itie, A. Polian, F. Baudelet, and J. Z. Jiang, *Appl. Phys. Lett.* **81**, 4820 (2002).

¹²Our more detailed SAD analysis has also shown that the strong diffraction pattern from wurtzite ZnO, as illustrated in the inset in Fig. 2(a), overlaps with low-intensity rings originating from amorphous SiO₂.

¹³J. C. Phillips, *Bonds and Bands in Semiconductors* (Academic, New York, 1973).

¹⁴H. M. Naguib and R. Kelly, *Radiat. Eff.* **25**, 1 (1975).

¹⁵An amorphous phase of ZnO can, however, be stabilized by impurities (such as Si), as has recently been discussed in detail in Ref. 16.

¹⁶S. O. Kucheyev, J. S. Williams, C. Jagadish, J. Zou, C. Evans, A. J. Nelson, and A. V. Hamza, *Phys. Rev. B* **67**, 094115 (2003).

¹⁷J. G. Chen, B. Frubberger, and M. L. Colaianni, *J. Vac. Sci. Technol. A* **14**, 1668 (1996).

¹⁸J.-H. Guo, L. Vayssieres, C. Persson, R. Ahuja, B. Johansson, and J. Nordgren, *J. Phys.: Condens. Matter* **14**, 6969 (2002).

¹⁹C. McGuinness, C. B. Stagarescu, P. J. Ryan, J. E. Downes, D. Fu, K. E. Smith, and R. G. Egdell, *Phys. Rev. B* **68**, 165104 (2003).

²⁰J. W. Chiou, J. C. Jan, H. M. Tsai, C. W. Bao, W. F. Pong, M.-H. Tsai, I.-H. Hong, R. Klausner, J. F. Lee, J. J. Wu, and S. C. Liu, *Appl. Phys. Lett.* **84**, 3462 (2004).

²¹Y. Sato, T. Mizoguchi, F. Oba, M. Yodogawa, T. Yamamoto, and Y. Ikuhara, *Appl. Phys. Lett.* **84**, 5311 (2004).

²²K. S. Hamad, R. Roth, J. Rockenberger, T. van Buuren, and A. P. Alivisatos, *Phys. Rev. Lett.* **83**, 3474 (1999).

²³L. Soriano, P. P. Ahonen, E. I. Kauppinen, J. Gomez-Garcia, C. Morant, F. J. Palomares, M. Sanchez-Agudo, P. R. Bressler, and J. M. Sanz, *Monatsh. Chem.* **133**, 849 (2002).

²⁴H. C. Choi, H.-J. Ahn, Y. M. Jung, M. K. Lee, H. J. Shin, S. B. Kim, and Y.-E. Sung, *Appl. Spectrosc.* **58**, 598 (2004).